Supplementary Material (ESI) for Lab on a Chip

Electronic Supplementary Information

Tuning Deterministic Lateral Displacement Devices Using Dielectrophoresis

Jason P. Beech, Peter Jönsson and Jonas O. Tegenfeldt

Experimental Setup

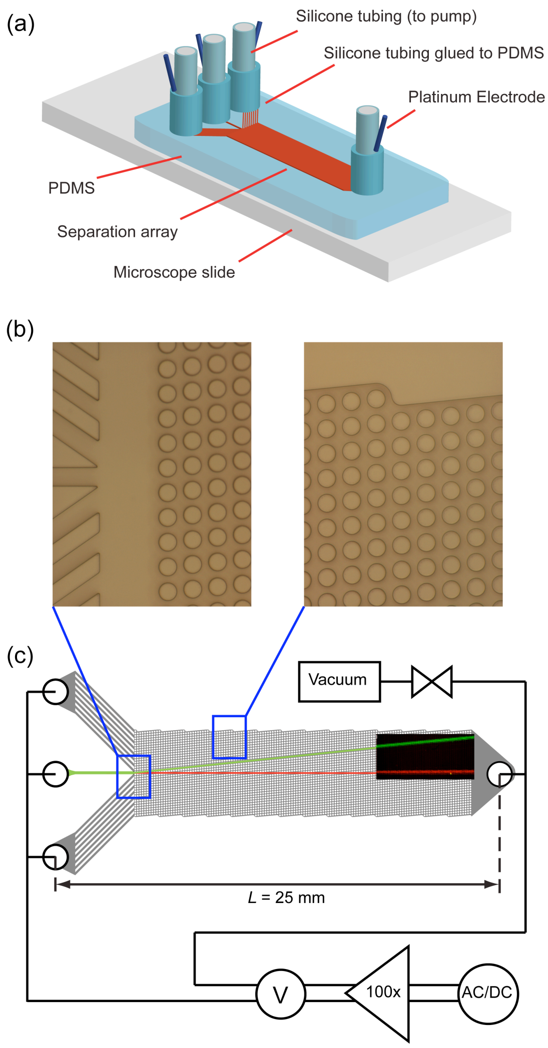

Fig. S1 Layout of the D-DLD with peripheral vacuum pump and electronic connections. **(a)** The device is fabricated in PDMS and glass using replica molding. **(b)** Micrographs of the entrance channels and a side-wall. **(c)** A scale drawing of the separation device. A stream of particles injected into the device is continuously separated about the critical diameter, D_c. Particles smaller than the critical diameter follow the direction of the fluid flow (red) whereas particles larger than the critical diameter follow the geometry of the post array (green). The black frame is a fluorescent micrograph (from movie m1.mov, ESI) showing actual separation of 3 µm (red) and 5 µm (green) diameter polystyrene beads. At this early stage the separated beads are extracted via a single exit for simplicity but for actual separation at least two exits will be used.

D_{c0} from Stretching Experiments

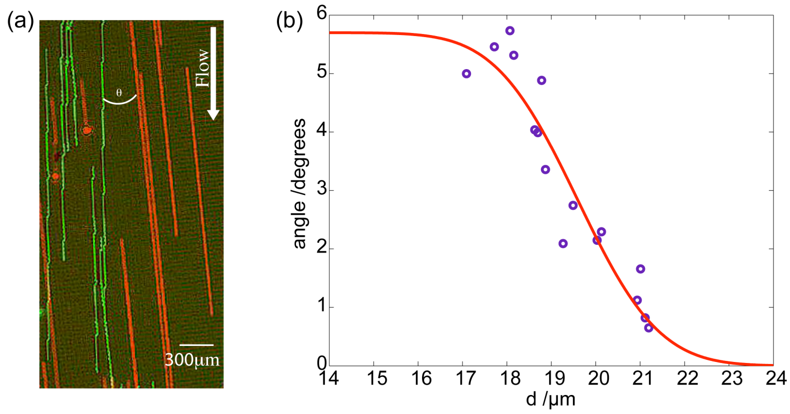

Fig. S2 (a) Two images are superimposed to show how 10μm diameter beads change from the displacement mode (red) to the zigzag mode (green) after stretching of the device. **(b)** The dependence of the migration angle of the beads through the device as a function of the gap size *d*. An angle of 5.7° corresponds to the red particle traces in (a) and 0° to the green traces.

We use an error function $5.7°/2 \cdot erf((d_c-d)/\Delta d)+5.7°/2$, where d is the gap size and d_c the critical gap at which half of the beads are in the zigzag mode and half are in the displacement mode, to estimate the correction factor α. We assume that when the beads are moving half in zigzag and half in bumping mode, the critical diameter in the device is equal to the mean radius of the beads which is 5 μm and we obtain:

$$\alpha = \frac{R_c N}{d} = \frac{5\ \mu\text{m} \cdot 10}{20\ \mu\text{m}} = 2.5 \qquad \text{(S1)}$$

The obtained value for α is then used in Eq. S2 to calculate D_{c0} in the present device.

$$D_{c0} = 2 \times \alpha \frac{d}{N} = 2 \times 2.5 \frac{12\ \mu\text{m}}{10} = 6\ \mu\text{m} \qquad \text{(S2)}$$

Simulations

Finite element simulations were made to model the flow and the electric field in the device. The simulations were performed separately in two steps using COMSOL Multiphysics® 3.4 (COMSOL AB, Stockholm, Sweden). The fluid flow was simulated in the device by solving the linear incompressible Navier-Stokes equation:

$$\begin{cases} 0 = -\nabla p + \eta \nabla^2 \boldsymbol{u} \\ 0 = \nabla \cdot \boldsymbol{u} \end{cases} \qquad \text{(S3)}$$

where p is the pressure, η the viscosity (= 1 mPa s) and $\boldsymbol{u}$ the flow velocity. To simulate the electric field Laplace's equation was solved (see Eq. S4).

$$-\nabla \cdot \left(\varepsilon_0 \varepsilon_r \nabla V \right) = 0 \qquad \text{(S4)}$$

where $\varepsilon_0 = 8.854 \cdot 10^{-12}$ F m^{-1}, ε_r is the relative permittivity ($\varepsilon_r \approx 80$ for pure water[1] and $\varepsilon_r \approx 2.5$ for PDMS[2]) and V is the electric potential.

Both Eqs. S3 and S4 are simplified expressions based on the following assumptions:

1) Neither the flow field nor the electric field is influenced by the particles.
2) The effect of the channel height on the electric field and the flow is neglected, thus the solutions to Eqs. S3 and S4 should be seen as the average fields the particles experience in the channel (the fields at the middle of the height of the channel).
3) The electric field distribution can be solved using an electrostatic model.[3]
4) Any build up of charge around the electrodes is negligible.

The smaller the particles are the less influence they will have on the flow and the electric field, but using particles with diameters on the order of half the gap width between the posts will most likely have an effect on the properties of the D-DLD. However, neglecting the effect of the particles will strongly reduce the complexity of the simulations. Even though the effect of the particle size should be kept in mind when comparing the simulated data with the experimental results, the current model is considered accurate enough to obtain quantitative information about the properties of the D-DLD.

The geometries of the two simulations are defined in Fig. S3, with the boundary conditions given in Table S1. The solutions for different pressure or voltage drops, respectively, were obtained by scaling the solutions obtained with the boundary conditions in Table S1.

Table S1. Boundary conditions for the flow and the electric field simulations. The numbering of the different boundaries are shown in Fig. S3 b and c for the flow and electric field simulations, respectively.

Flow simulation		*Electric field simulation*	
1.	$\boldsymbol{u}_1 = \boldsymbol{u}_2$, $p_2 = p_1 + 0.03276$ Pa*	**1.**	$V_1 = V_2$
2.	$\boldsymbol{u}_1 = \boldsymbol{u}_2$, $p_2 = p_1 + 0.03276$ Pa*	**2.**	$V_1 = V_2$
3.	$\boldsymbol{u}_3 = \boldsymbol{u}_4$, $p_3 = p_4 + 0.5157$ Pa**	**3.**	$V_3 = V_4 + 0.336$ V***
4.	$\boldsymbol{u}_3 = \boldsymbol{u}_4$, $p_3 = p_4 + 0.5157$ Pa**	**4.**	$V_3 = V_4 + 0.336$ V***
5.	$\boldsymbol{u}_5 = \boldsymbol{0}$		

* A lateral pressure drop to ensure that 1/10th of the flow exits through boundary 1.

** A constant pressure drop along the device yielding a mean velocity of 190 μm s^{-1} for a particle following the flow (without diffusion).

*** Corresponds to a voltage drop of 100 V over the 25 mm long device giving an average electric field E=40 V cm^{-1}.

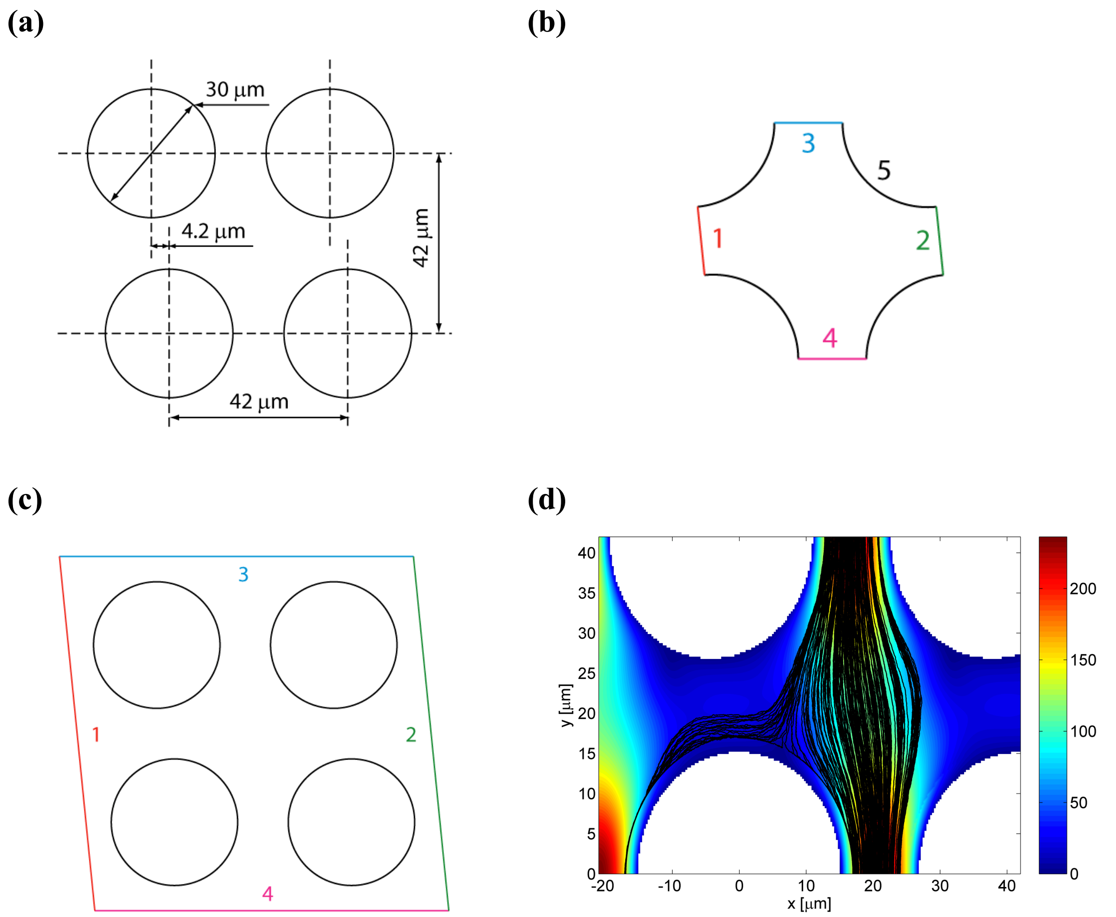

Fig. S3 (a) Dimensions of the post array in the D-DLD device. **(b)** The geometry used in the simulation of the fluid flow. **(c)** The geometry used to simulate the electric field in the D-DLD device. In both cases the black boundaries correspond to the posts. The boundary conditions are presented in Table S1. **(d)** 200 simulated particle trajectories for beads with $D_{\mathrm{eff}} = D\times4.7/6.0 = 5$ µm moving at 90 µm s^{-1}. The start position for each trajectory corresponds to the end position for the previous trajectory (translated from the bottom to the top of the shown geometry). The first trajectory starts at the top right position next to the post.

A particle will move with the flow in the device unless acted on by a force. In the D-DLD this force may have two different origins. It may be due to the particle hitting a post or may arise from the dielectrophoretic force. In the latter case a viscous drag force, $\boldsymbol{F}_{\mathrm{drag}}$, which in steady state is balanced by the dielectrophoretic force, $\boldsymbol{F}_{\mathrm{DEP}}$, will also slow the particle down, thus yielding:

$$\boldsymbol{F}_{\mathrm{drag}} = \boldsymbol{F}_{\mathrm{DEP}} = 3\pi\eta D\left(\boldsymbol{u} - \boldsymbol{u}_{\mathrm{flow}}\right) \tag{S5}$$

where η is the viscosity of the fluid, D the particle radius, $\boldsymbol{u}$ the resulting particle velocity and $\boldsymbol{u}_{\mathrm{flow}}$ the flow velocity of the fluid at the position of the particle. Rearranging Eq. S5 then yields

$$\boldsymbol{u} = \boldsymbol{u}_{\mathrm{flow}} + \boldsymbol{F}_{\mathrm{DEP}}/\left(3\pi\eta D\right) \tag{S6}$$

In Eq. S6 both $\boldsymbol{u}_{\mathrm{flow}}$ and $\boldsymbol{F}_{\mathrm{DEP}}$ are functions of the position in the device. $\boldsymbol{u}_{\mathrm{flow}}$ is obtained directly from the finite element simulations whereas Eq. 2b in the main manuscript is used to calculate $\boldsymbol{F}_{\mathrm{DEP}}$ together with the simulation of the electric field.

In calculating $\boldsymbol{F}_{\mathrm{DEP}}$ the medium permittivity, ε_{m}, was set to $\varepsilon_{\mathrm{m}} = 80\varepsilon_0$, where ε_0 is the vacuum permittivity.[1] The value of $\mathrm{Re}(f_{\mathrm{CM}})$ was set to -0.49 in the simulations.
Because of the periodicity of the array, the simulations of the particle trajectories are performed over the part of the array seen in Fig. S3d only. Particles leaving the bottom of the cell are reintroduced with the same relative lateral position at the top. The particle trajectory simulation is begun by first choosing a start position, (x,y), for the particle, here chosen as one particle radius from the top right post. $\boldsymbol{u}_{\mathrm{flow}}$ and $\boldsymbol{F}_{\mathrm{DEP}}$ are calculated at this position and the velocity is obtained from Eq. S6. A new (x,y)-position is then calculated as $(x,y) = (u_{\mathrm{x}},u_{\mathrm{y}})\cdot\mathrm{d}t$ where $\mathrm{d}t$ is a small time increment. The step length was set sufficiently small so that neither $\boldsymbol{u}_{\mathrm{flow}}$ nor $\boldsymbol{F}_{\mathrm{DEP}}$ change significantly over the distance moved. Particle-post interactions were handled such that if the new (x,y)-position of a particle was nearer to a post than one particle radius then the particle was moved so that the new position was one radius from the surface of the post. Diffusion was also included by adding, for each time step $\mathrm{d}t$, a normally distributed random displacement in both the x- and y-directions with an expectation value of 0 and a standard deviation of $(2D_{\mathrm{diff}}\times\mathrm{d}t)^{1/2}$, where D_{diff} $(= \mathrm{k_B}T/(3\pi\eta D))$ is the diffusion coefficient of the particle with $\mathrm{k_B}$ being Boltzmann's constant, T the temperature and η the viscosity of the bulk fluid.

All simulations were done for 200 rows of posts after which the angular deflection and the mean velocity were calculated over a period of 180 posts, where the first 15 and last 5 trajectories were omitted so that the choice of the starting position did not influence the results. All particle simulations were made using MATLAB® 2007b (The MathWorks™, Natick, MA, USA).

Theoretical Model

Let x denote the distance from the left post and outward. $\boldsymbol{F}_{\mathrm{DEP}}(x)$ can then be expanded in a series solution in x, where only the first two terms are kept here for simplicity, yielding:

$$F_{\mathrm{DEP}}(x) \approx C\varepsilon_{\mathrm{m}}D^3\left(-\mathrm{Re}\left(f_{\mathrm{CM}}\right)\right)\langle E\rangle^2\left(1 - x/w\right),\ 0 < x < D_{\mathrm{c0}}/2 \qquad \text{(S7)}$$

where C and w are (for nDEP) positive constants which can be determined from the dielectrophoretic force nearest a post and how fast this force decreases when moving away from the post, respectively. These two parameters depend on the dimensions and properties of the channel and the bulk fluid. L is the length of the channel, D the particle diameter and E is the average, root mean square, electric field over the channel. The displacement velocity, v_{DEP}, due to the dielectrophoretic force is given by:

$$v_{\mathrm{DEP}}(x) = F_{\mathrm{DEP}}(x)/(3\pi\eta D) \qquad \text{(S8)}$$

so that

$$v_{\mathrm{DEP}}(x) = \frac{C\varepsilon_{\mathrm{m}}D^2\left(-\mathrm{Re}\left(f_{\mathrm{CM}}\right)\right)}{3\pi\eta}E^2\left(1 - x/w\right) \qquad \text{(S9)}$$

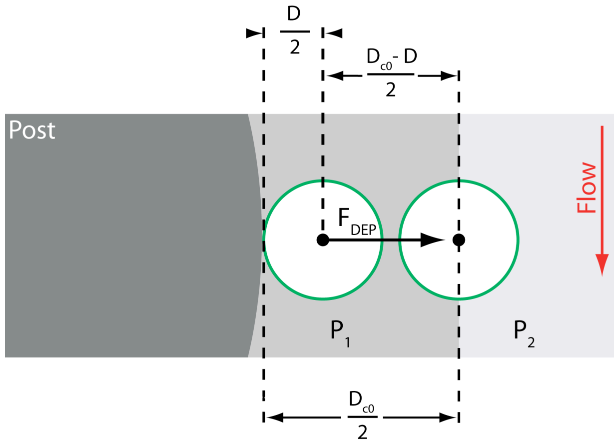

Fig. S4 (a) The distance that a particle of diameter D needs to be displaced by the DEP force in order to behave like a particle larger than the critical size.

The distance, dx, that a particle is displaced, perpendicular to the fluid flow, during the time dt is given by:

$$\mathrm{d}x = v_{\mathrm{DEP}}\mathrm{d}t \tag{S10}$$

For a particle of diameter D to switch from the zigzag to the bumping mode its hydrodynamic center of mass needs to be moved out of the flow at P_1 and into P_2, see Fig S4. In order for this to occur a particle of diameter D needs to move a distance corresponding to $(D_{c0}\text{-}D)/2$, where D_{c0} is the width of the stream at P_1, which is equivalent to the critical diameter of the device without an applied voltage.. The time, τ, this would take is:

$$\tau = \int_{D/2}^{D_{c0}/2} \frac{\mathrm{d}x}{v_{\mathrm{DEP}}(x)} = \frac{3\pi\eta w \times \ln\left(1 + (D_{c0} - D)/(2w - D_{c0})\right)}{C\varepsilon_{\mathrm{m}} D^2 \times \left(-\mathrm{Re}(f_{\mathrm{CM}})\right) E^2} \tag{S11}$$

τ will depend on the time it takes for a particle to pass between two posts. This time is expected to be inversely proportional to the flow velocity or equivalently inversely proportional to the mean particle velocity, v, at zero voltage ($\tau = B/v$, with B a characteristic distance over which the particle can be displaced due to the dielectrophoretic force). The average electric field, E_{c}, required to make $D_{\mathrm{c}} = D$ is then:

$$E_{\mathrm{c}} = \frac{\sqrt{A \times v}}{\sqrt{\left(-\mathrm{Re}(f_{\mathrm{CM}})\right)}} \times \frac{\sqrt{\ln\left(1 + \beta^{-1}(D_{c0} - D_{\mathrm{c}})\right)}}{D_{\mathrm{c}}} \tag{S12}$$

where the constants

$$A = \frac{3\pi\eta w}{C\varepsilon_{\mathrm{m}} B} \text{ and } \beta = 2w - D_{c0} \tag{S13}$$

have been introduced to simplify the expression in Eq. S12.

During the time τ a spherical particle with the diameter D_c will on average diffuse a distance of the order Δx_d:

$$\Delta x_\mathrm{d} = \sqrt{2D_\mathrm{diff}\tau} \tag{S14}$$

where $D_{diff} = k_B T/(3\pi\eta D_c)$ is the diffusion coefficient of the spherical particles.

To model the effect diffusion has on the transition width from the zigzag to the bumping mode the average electric field, $E_c \pm \Delta E_c$, required to move a particle the distance $(D_{c0}-D_c)/2 \pm \Delta x_d$ in a time τ is determined as:

$$\begin{aligned}\tau &= \int_{D_\mathrm{c}/2}^{D_\mathrm{c0}/2\pm\Delta x_\mathrm{d}} \frac{\mathrm{d}x}{v_\mathrm{DEP}(x)} \approx \int_{D_\mathrm{c}/2}^{D_\mathrm{c0}/2} \frac{\mathrm{d}x}{v_\mathrm{DEP}(x)} \pm \frac{\Delta x_\mathrm{d}}{v_\mathrm{DEP}(D_\mathrm{c0}/2)} = \\ &= \frac{3\pi\eta w}{C\varepsilon_\mathrm{m} D_\mathrm{c}^2 \times \left(-\mathrm{Re}(f_\mathrm{CM})\right)\left(E_\mathrm{c} \pm \Delta E_\mathrm{c}\right)^2} \times \left(\ln\left(1+\beta^{-1}(D_\mathrm{c0}-D_\mathrm{c})\right) \pm \frac{C}{K} \times \frac{\Delta x_\mathrm{d}}{w}\right)\end{aligned} \tag{S15}$$

where Eq. S9 has been used for the definition of $v_{DEP}(x)$ and a new constant K has been introduced as a measure of the magnitude of $v_{DEP}(D_{c0}/2)$ according to:

$$v_\mathrm{DEP}(D_\mathrm{c0}/2) = \frac{K\varepsilon_\mathrm{m} D_\mathrm{c}^2\left(-\mathrm{Re}(f_\mathrm{CM})\right)}{3\pi\eta} E_\mathrm{c}^{\ 2} \tag{S16}$$

The reason for introducing K is to obtain a more accurate value for the DEP velocity close to D_{c0} than would be the case if using the series expansion expression in Eq. S9, which averages over all values of x. In Eq. S15 it has also been assumed that v_{DEP} changes negligibly over the distance the particles diffuse. Without diffusion the average electric field, E_c, required to move the particle the distance $(D_{c0}-D_c)/2$ in a time τ is:

$$\tau = \int_{D_\mathrm{c}/2}^{D_\mathrm{c0}/2} \frac{\mathrm{d}x}{v_\mathrm{DEP}(x)} = \frac{3\pi\eta w \times \ln\left(1+\beta^{-1}(D_\mathrm{c0}-D_\mathrm{c})\right)}{C\varepsilon_\mathrm{m} D_\mathrm{c}^2 \times \left(-\mathrm{Re}(f_\mathrm{CM})\right) E_c^{\ 2}} \tag{S17}$$

Setting Eqs. 15 and 17 equal yields that the transition width, ΔE_c, is given by:

$$\Delta E_\mathrm{c} \approx \frac{C}{2K} \times \frac{\Delta x_\mathrm{d}}{w} \times \frac{1}{\ln\left(1+\beta^{-1}(D_\mathrm{c0}-D_\mathrm{c})\right)} \times E_\mathrm{c} \tag{S18}$$

where it has been assumed that $\Delta E_c << E_c$. Δx_d is given by Eq. S14 and since the time for diffusion, t_d, should be inversely proportional to the average particle velocity in the device, v, at zero voltage, Eq. S18 can finally be rewritten as:

$$\Delta E_\mathrm{c} \approx \frac{\sqrt{\chi \times (D_\mathrm{c} v)^{-1}}}{\ln\left(1+\beta^{-1}(D_\mathrm{c0}-D_\mathrm{c})\right)} \times E_\mathrm{c} \tag{S19}$$

where χ, with the same units as diffusion, is a material parameter, introduced to simplify the expression in Eq. S19, which is given by

$$\chi \approx \frac{C^2 B}{6K^2 w} \times \frac{\mathrm{k_B} T}{\pi \eta w} \tag{S20}$$

Particle tracking

The analysis of the particle trajectories and velocities through the device was performed in MATLAB® 2007b (The MathWorks™, Natick, MA, USA) using a custom-written script. The images, stored as a stack of tif files, were first imported into the program and low-pass filtered using a Gaussian convolution of each image. Next an intensity threshold, set to 10% of the maximum intensity value in the images, was used to discriminate between the particles (intensity above the threshold) and the background (intensity below the threshold). The correct detection of particles was also verified visually. To further improve the discrimination between background and particles only regions consisting of at least three connected pixels, with intensities over the threshold value, were considered as detected particles. The centroid position of each detected particle was subsequently stored for each frame for further analysis.

To determine the angle the particles travel in the device two regions parallel to the flow direction were defined each corresponding to a distance of ten posts (equal to the period of the device). The first region was placed at the image side corresponding to the inlet whereas the second region was placed at the image side corresponding to the outlet. The relative number of particles, $n(y)$, in each region at or above a height y over a line parallel to the flow direction, was calculated next. An error function according to Eq. S21 was then fitted to $n(y)$ yielding the average position of the particles at each region and the width, Δy, of the particle distribution:

$$n(y) = 0.5 \times \left(1 - \mathrm{erf}\left((y - y_0)/\Delta y\right)\right) \tag{S21}$$

The angle at which the particles were travelling was then determined from the difference in $n(y)$ for the outlet and inlet regions divided by the distance between the two regions.

To calculate the mean velocity of the particles, the position of each particle in the subsequent frame needed to be determined. This was performed by comparing the position of each particle in frame N to the position of all particles in frame N+1. The particle that was closest in frame N+1, and positioned in the flow direction, was assumed to be the same particle as in frame N, thus yielding the distance the particle had travelled between the two frames. The correct tracking of the particles were also verified visually. By averaging the travelled distance obtained from all frames and particles, the mean velocity of the particles could then be determined since the time between two successive frames was known.

References

1. "Physical Constants of Organic Compounds", in CRC Handbook of Chemistry and Physics, 88th Edition (Internet Version 2008), David R. Lide, ed., CRC Press/Taylor and Francis, Boca Raton, FL.

2. http://web.mit.edu/6.777/www/matprops/pdms.htm, Accessed 2007-11-07, 2007.

3. N. G. Green and H. Morgan, *J Phys D Appl Phys*, 1997, 30, 2626-2633.